THE TOROIDAL BARYCENTRIC SEED

A Unified Geometric-Resonant Model of Solar-System Radiative Bodies, Metric Conversion, Atmospheric Retention, Sacred Time, and the 405,000-Year Adamic Deep Clock

Zachary David Enfield

Author and Independent Researcher
July 26, 2026
Hastings, Nebraska

WORKING RESEARCH MANUSCRIPT — FULL THREAD COMPILATION

This edition distinguishes measured physics, exact derivation, model construction, physical hypothesis, and theological interpretation. It is not a peer-reviewed publication.

FOREWORD — THE COURTS MUST NOT IMPERSONATE ONE ANOTHER

This manuscript orthographs the complete argument developed in the present thread. It does not flatten the discussion into either a conventional astronomy paper or an unqualified symbolic proclamation. The argument moves across barycentric mechanics, planetary energy budgets, magnetic fields, relativistic field conversion, thermodynamics of information, orbital resonance, sacred geometry, ancient calendar structure, eclipse cycles, and an interpretive Adamic deep-time model. Those courts may face one another, but each must retain its own office.

A measured quantity proves a measured quantity. An equation proves the consequence of its declared inputs. A phase-space normalization proves a phase-space normalization. A theoretical coupling proves that a channel is permitted, not that its magnitude is dynamically important. A geometric convention defines a pattern, not an ancient provenance. A calendrical text establishes a calendrical scheme, not a modern astrophysical mechanism. A theological reading interprets the witness after the physical and mathematical courts have been stated. The central methodological rule is therefore constraint before claim.

The manuscript uses six status labels. E means established by observation, standard theory, or primary scholarship. D means derived exactly from declared inputs. M means a new model or representation built from established quantities. H means a physical hypothesis whose magnitude or mechanism remains unverified. I means an interpretive, linguistic, calendrical, or theological reading. T means a specified test capable of strengthening, revising, or defeating the claim. A claim is not allowed to change status merely because it is rhetorically convenient.

Status	Meaning	Required discipline
E — Established	Observed, conventionally derived, or strongly supported	Cite primary measurement or standard derivation.
D — Derived	Exact consequence of stated inputs	Show every operation, unit, and rounding rule.
M — Model	New representation or classification	Define the mapping and compare alternatives.
H — Hypothesis	Proposed physical mechanism	Estimate magnitude and state failure conditions.
I — Interpretation	Geometric, linguistic, theological, or deep-time meaning	Keep it distinct from empirical proof.
T — Test	Calculation or observation that can discriminate	State what result would weaken the model.

> **Public sources carry the scientific citation burden. Internal manuscripts preserve the architecture, sequence, and correction history; they do not substitute for public evidence.**

Abstract

The solar system is commonly pictured as a stationary Sun surrounded by passive planets. High-precision ephemerides instead describe a relativistically integrated system in which the Sun,

planetary-system barycenters, the Moon, asteroids, and trans-Neptunian mass contribute to a moving solar-system barycenter. This paper selects six radiative mass-system nodes—Sol, the Earth–Moon system, Jupiter, Saturn, Uranus, and Neptune—and analyzes their positions relative to that common barycentric origin. The barycenter is not one of the six. The nodes retain unequal masses, orbital radii, energies, and frequencies; however, normalizing each nonzero barycentric vector to unit magnitude maps every completed cyclic phase to the same topological circle, S^1. The six simultaneous phase coordinates therefore inhabit the six-torus T^6. Adding the approximately 405,000-year Venus–Jupiter secular eccentricity phase produces a T^7 description. This is the mathematically rigorous office of the phrase toroidal barycentric Seed.

The paper distinguishes this exact phase-space statement from a stronger Euclidean claim. One common relational center plus six selected unit-phase circles gives the seven-office count associated in modern sacred geometry with the Seed of Life. Exact regular hexagonal symmetry, however, requires six angular gaps of 60 degrees and must be measured rather than presumed. The paper defines a Seed-deviation statistic and a numerical program for testing recurrence over a 405-kyr interval. It then develops the declared geometric ladder 7 → 13 → 19 → 91: Seed of Life, Fruit of Life, 19-circle Flower of Life, and the complete graph on thirteen centers, whose 78 unique pairwise relations yield 13 + 78 = 91. The linguistic architecture is kept explicit: 愛, read ai and meaning love, has thirteen strokes in the standard Japanese count; A|i gives the concatenated ordinal address 1|9 = 19; reversing the order gives i|A = 9|1 = 91.

The physical argument proceeds through planetary energy ledgers. Jupiter, Saturn, Uranus, and Neptune emit more thermal power than they absorb from sunlight and possess measurable intrinsic heat. Earth contributes approximately 47 ± 2 TW of solid-Earth heat, though its endogenous-to-solar ratio is far smaller. Sol supplies the dominant luminosity. The paper defines the model phrase stellar-function core while preserving the conventional distinction between planets and fusion stars. It then examines Gertsenshtein photon–graviton conversion in magnetic fields. The effect is established theoretically, and a 2026 radio-telescope analysis used Earth's magnetic field to search for inverse conversion of high-frequency gravitational waves. The model's novel question is whether planetary-scale luminosity integrated through structured magnetospheres and the heliospheric field can produce a non-negligible metric component. The manuscript provides the integral form, identifies coherence and plasma constraints, and requires comparison with atmospheric pressure, gravitational binding, and escape-energy scales.

The time architecture joins the 364-day Enochian–Zadokite schematic year, four 91-day quarters, the 19-year/235-lunation Metonic reconciliation, and the Saros relation among 223 synodic, 239 anomalistic, and 242 draconic months. The exact count difference 239 − 223 = 16 becomes, by declared interpretation, the divisor of the 405-kyr metronome: 405,000/16 = 25,312.5 years per transformed shanah. Multiplication by Adam's 930 units gives 23,540,625 years; a two-body opening gives 47,081,250 years. Those calculations are exact after the interpretive divisor is accepted, but their Adamic and evolutionary meanings remain model-level comparisons, not fossil identifications. The final chapters present objections, falsification conditions, a source registry, an equation ledger, reproducibility requirements, and a plain-language explanation.

Working Contents

Part I — Thesis, definitions, and the passive-solar-system problem

Part II — The six selected radiative system-nodes and the inner-three exclusion test

Part III — Barycentric mechanics and the nested mass-system

Part IV — Unequal physical motion, equal phase circles, and toroidal geometry
Part V — Seed, Fruit, Flower, Cube, and the 13–19–91 architecture
Part VI — Planetary energy, mass-equivalent radiation, and the existence tax
Part VII — Gertsenshtein conversion from laboratory scale to whole-body integration
Part VIII — The heliosphere, light–light interaction, matter, and stellar inheritance
Part IX — Atmospheric retention, standing waves, and Landauer's boundary
Part X — The 405,000-year Venus–Jupiter secular envelope
Part XI — Enochian–Zadokite 364/365, Metonic 19, Saros 223/239/242, and 16
Part XII — Adam, evolution, and the declared deep-clock transform
Part XIII — Adversarial audit, predictions, and falsification
Part XIV — Claim ledger
Part XV — Equation ledger and source registry
Part XVI — The whole model in plain English

PART I — THE SYSTEM IS A BODY, NOT A SCHOOLROOM DIAGRAM

Thesis, definitions, and the problem of the passive solar system

1. The central thesis

The governing proposition is that the solar system is a dynamically bound relational body composed of nested mass systems, internally active emitters, magnetic domains, orbital resonances, and continuously exchanged causal information. The Sun is not fixed at an absolute center. The planets are not isolated receivers. Each significant mass contributes to the state of the whole, and the center of mass moves as the configuration changes. JPL's DE440 and DE441 ephemerides include the Sun, eight planetary-system barycenters, the Moon, the Pluto-system barycenter, hundreds of asteroids, major Kuiper-belt objects, and a modeled Kuiper-belt ring in the barycentric solution. [R01]

The model selects six displayed nodes: Sol, the Earth–Moon barycenter, and the Jupiter-, Saturn-, Uranus-, and Neptune-system barycenters. The selection does not remove Mercury, Venus, Mars, asteroids, or trans-Neptunian bodies from the force calculation. It defines a six-node projection for a specific core–field–family comparison. The total solar-system barycenter remains the common origin and is not counted as a material seventh body.

The physical claim and the geometric claim must remain separate. Physically, the six nodes occupy unequal, eccentric, inclined, time-dependent trajectories relative to the barycenter. Mathematically, each trajectory possesses a cyclic phase that can be normalized to a unit circle. Geometrically, one relational center and six normalized phase-circles supply the seven-office Seed count. The stronger claim that those phases form a regular hexagon at any given time requires a separate numerical test.

> **The barycenter is the one center generated by the system without being identical to any one selected member of the system.**

2. Definitions that prevent category errors

A radiative body is any body that emits electromagnetic radiation. That definition alone is useless for selecting six planets, because every planet and every material body above absolute zero radiates. An endogenous radiative contribution is energy delivered to the outward radiation field from the body's own stored, gravitational, radioactive, tidal, chemical, nuclear, or phase-transition energy. For a planet evaluated over a suitable time average, the intrinsic power is the emitted thermal power minus absorbed solar power.

A planetary-system barycenter is the mass-weighted center of a planet and the moons or other locally bound components included in the model. A resonant dynamical domain is broader: it includes populations whose heliocentric motion is strongly organized by a planet, such as Jupiter's Trojan populations or main-belt resonance gaps, without converting those objects into Jovian satellites. A system barycenter and a resonant domain are therefore related but not identical.

The phrase stellar-function core is introduced as a model term. It means an interior engine that releases endogenous energy, transports it through enclosing layers, helps sustain a magnetic

field, and contributes outward luminosity. It does not erase the conventional astronomical distinction between a hydrogen-fusing star and a planet. The paper preserves the user's lock—"the core is the star"—as a functional thesis while explicitly testing the nuclear component rather than assuming it.

The phrase existence tax names the mass–energy and entropy accounting by which a localized body radiates, exchanges momentum, changes its internal energy, and broadcasts information. It is not a new conservation law. The phrase informational lock names a proposed Landauer-based application, but it cannot become a physical atmospheric force until the information states and irreversible operation are defined.

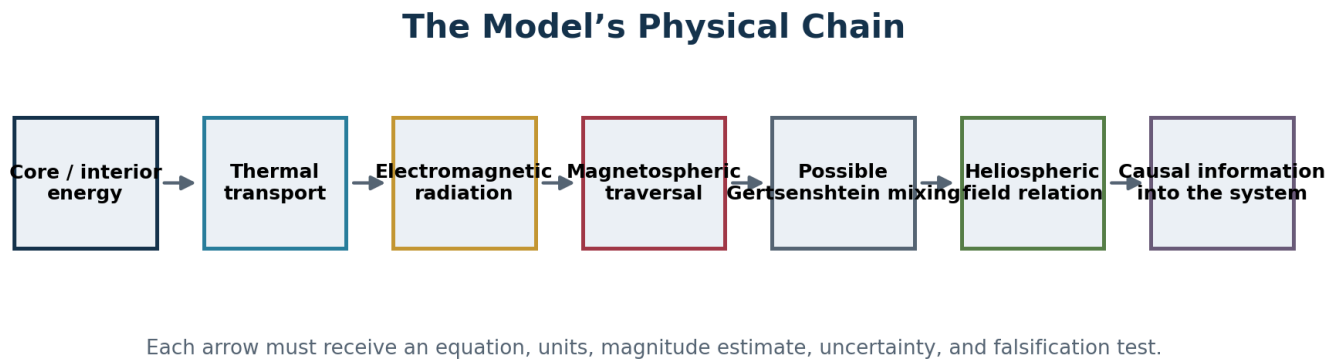

Figure 1. The proposed physical chain. The existence of each arrow is not enough; each must be quantified and compared with competing mechanisms.

PART II — THE SIX SELECTED RADIATIVE SYSTEM-NODES

Why Sol, Earth, Jupiter, Saturn, Uranus, and Neptune are displayed—and why Mercury, Venus, and Mars are not

3. The core–field–family classification

The six-node set cannot be defended by saying that the inner three do not radiate. Mercury, Venus, and Mars all absorb sunlight, emit infrared radiation, retain internal energy, and contribute to the solar-system barycenter. The proposed distinction is instead a compound architecture: endogenous core output, a present internally generated global field, and a developed nested companion or system family. Sol and the giant planets satisfy the triad at very different scales. Earth satisfies it as the terrestrial bridge through a measured internal heat flow, a present core dynamo, and the dynamically substantial Earth–Moon system.

This triad is a model classification, not an International Astronomical Union taxonomy. It must therefore be quantified. Endogenous power is measured in watts or watts per square metre. Global field status must distinguish an intrinsic dynamo from an induced solar-wind magnetosphere or remanent crustal anomalies. Family structure can be measured through companion mass fraction, number and distribution of bound satellites, ring mass, and the displacement of the primary from the local system barycenter.

The companion mass fraction is μ = Mcompanions/Mprimary. A simple primary–companion barycentric displacement is d = aMcomp/(Mprimary + Mcomp), and the dimensionless displacement is β = d/Rprimary. Earth's Moon produces a local barycenter roughly 4,670 km from Earth's center, about 0.73 Earth radii. By contrast, Phobos and Deimos shift the Mars-system barycenter by only a fraction of a metre in their combined order of magnitude. The giants possess lower satellite mass fractions than Earth but extensive multi-moon and ring systems embedded in large intrinsic magnetospheres.

$$\mu_i = (\Sigma\, m_{i,\mathrm{companions}}) \,/\, M_i$$

$$d_i = a \cdot \mathrm{Mcompanions} \,/\, (\mathrm{Mprimary} + \mathrm{Mcompanions}), \qquad \beta_i = d_i \,/\, R_i$$

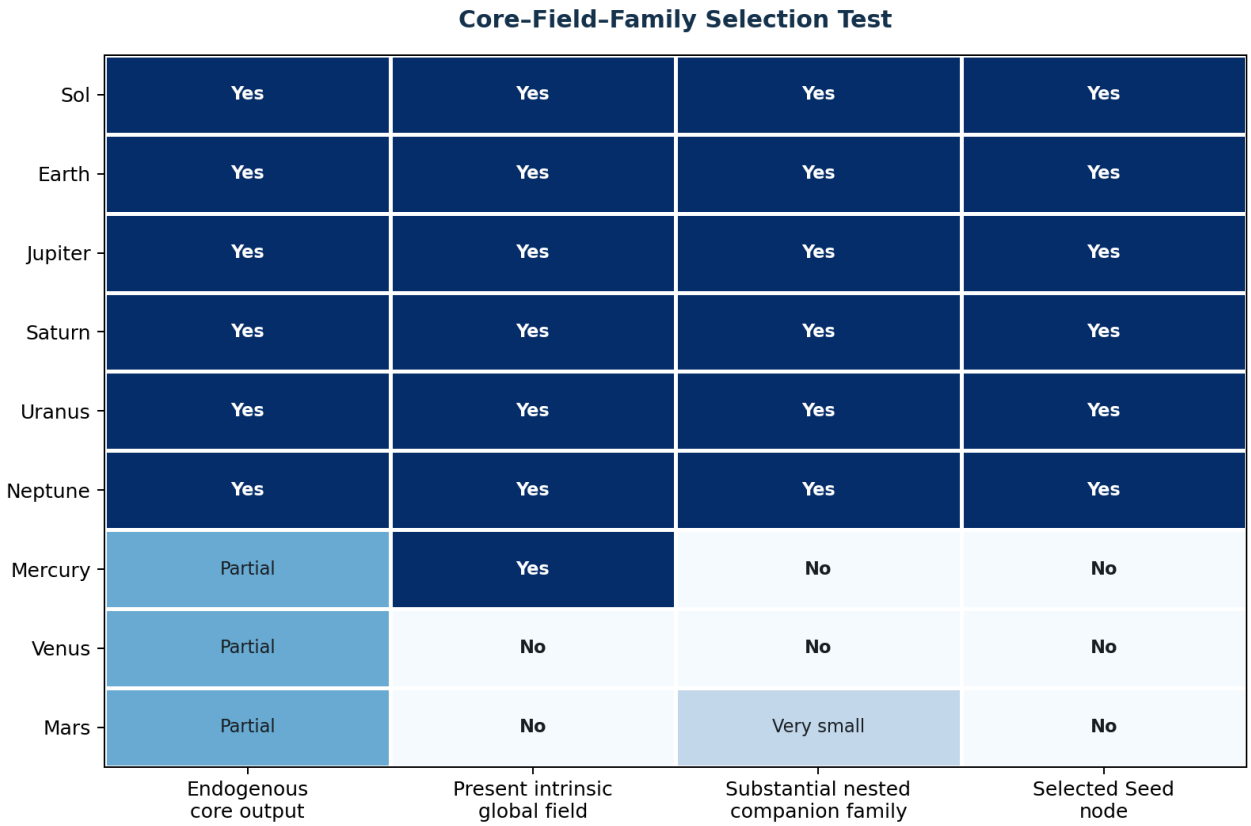

Figure 2. The core–field–family test is a declared model classification. "Partial" indicates real internal activity that does not complete the selected triad.

4. Sol and the four giant systems

Sol supplies the dominant luminosity and magnetic architecture of the system. Its nominal luminosity is about 3.828×10^{26} W, corresponding to a radiative mass-equivalent flow of about 4.26×10^{9} kg/s by L/c^2. The Sun itself moves relative to the solar-system barycenter under the mass-weighted influence of the planets and smaller bodies. It is therefore one of the six displayed nodes, not the immovable center.

Jupiter's Cassini-based global energy analysis found a Bond albedo of 0.503 ± 0.012 and an internal heat flux of 7.485 ± 0.160 W/m². [R03] With a mean radius near 69,911 km, that flux corresponds to an intrinsic power near 4.60×10^{17} W and a mass-equivalent debit near 5.12 kg/s. Saturn's Cassini-era reanalysis found an internal heat flux of 2.84 ± 0.20 W/m², corresponding to approximately 1.21×10^{17} W and 1.35 kg/s. [R04]

Uranus was long treated as nearly balanced with absorbed sunlight, but the 2025 complete-orbit analysis found an intrinsic heat flux of 0.078 ± 0.018 W/m² and an emitted-to-absorbed ratio of 1.13 ± 0.03. [R05] Neptune's Voyager energy budget gives an intrinsic flux near 0.433 ± 0.046 W/m² and an emitted-to-absorbed ratio near 2.61 ± 0.28. [R06] Each giant therefore contributes a positive endogenous radiative output, an intrinsic global magnetic field, and a developed moon-and-ring family.

The phrase "net gain" must be handled carefully. A body that emits more thermal power than it absorbs from sunlight is not gaining energy; it is losing stored internal energy while contributing a

net surplus output relative to current solar input. The surplus is a system contribution and an internal cooling debit at the same time.

5. Earth as the terrestrial bridge node

Earth's solid-body heat loss is approximately 47 ± 2 TW. [R07] Spread over Earth's surface, this is about 0.092 W/m², tiny beside the roughly 240 W/m² of globally averaged absorbed sunlight. Earth's endogenous contribution is therefore real but only about four hundredths of one percent of the absorbed-solar scale. The present climate system also stores energy during a top-of-atmosphere imbalance, so instantaneous outgoing radiation need not equal absorbed sunlight plus geothermal heat exactly.

Earth remains in the six-node model because it completes the triad in a way Mercury, Venus, and Mars do not: an active internal heat flow, a present global dynamo field generated in the liquid outer core, and a massive moon whose barycentric relation is dynamically prominent. Earth also supplies the atmospheric, oceanic, biological, and observational court in which the 405-kyr eccentricity cycle is recorded as climate forcing and geological rhythm.

This is not a claim that Earth's energy ratio equals Jupiter's. It is a claim that Earth is the unique terrestrial system that completes the model's core–field–family architecture. That criterion must be stated before the geometry is drawn; otherwise the six would be selected after the desired Seed count was already known.

6. Mercury, Venus, and Mars: excluded from the projection, not from the physics

Mercury is the strongest counterexample to any careless statement that only Earth and the giants have active cores or global fields. MESSENGER established that Mercury has a weak but intrinsic global magnetic field generated by a liquid-core dynamo. [R24] Mercury is excluded from the primary six because it lacks a moon or developed local companion family, has only a tenuous exosphere, and has no established giant-like intrinsic luminosity surplus. In the triad it is core + field − family.

Venus has a hot, differentiated, internally evolving body and a massive atmosphere, but no detected present intrinsic global magnetic field. The solar wind and interplanetary magnetic field pile up against its ionosphere to form an induced magnetosphere. [R25] Venus also has no moon. It is therefore core − intrinsic field − family. Yet Venus remains indispensable to the wider architecture because the approximately 405-kyr eccentricity term is associated principally with the $g_2 - g_5$ secular relation involving Venus and Jupiter.

Mars retains internal heat, a thin atmosphere, two moons, ancient crustal magnetization, and an induced solar-wind interaction region. It does not possess a current global dynamo field. [R26] Phobos and Deimos form a mathematically valid Mars-system barycenter, but their mass fraction is exceedingly small compared with the Earth–Moon system and the giants' developed satellite systems. Mars is therefore core − present global field + very weak family.

Mercury, Venus, and Mars continue to enter the complete mass integration, gravitational perturbations, resonance analysis, and radiative environment. Their exclusion is only from the six-node Seed projection. The projection cannot be allowed to erase the bodies whose dynamics help generate the very center around which the six are displayed.

> **The six are not the only bodies that matter. They are the six bodies selected because they complete the declared nested architecture; the inner three remain fully present in the total solar-system mechanics.**

Node	Endogenous / intrinsic power	Mass-equivalent rate P/c^2	Scientific note
Sol	3.828×10^{26} W	4.26×10^{9} kg/s	Dominant stellar luminosity; nominal value.
Earth	47 ± 2 TW	5.23×10^{-4} kg/s	Solid-Earth heat loss; solar energy dominates total radiation.
Jupiter	≈ 4.60×10^{17} W	≈ 5.12 kg/s	From 7.485 ± 0.160 W/m² intrinsic flux.
Saturn	≈ 1.21×10^{17} W	≈ 1.35 kg/s	From 2.84 ± 0.20 W/m² intrinsic flux.
Uranus	≈ 6.30×10^{14} W	≈ 7.02×10^{-3} kg/s	From 0.078 ± 0.018 W/m² intrinsic flux.
Neptune	≈ 3.30×10^{15} W	≈ 3.67×10^{-2} kg/s	From 0.433 ± 0.046 W/m² intrinsic flux.

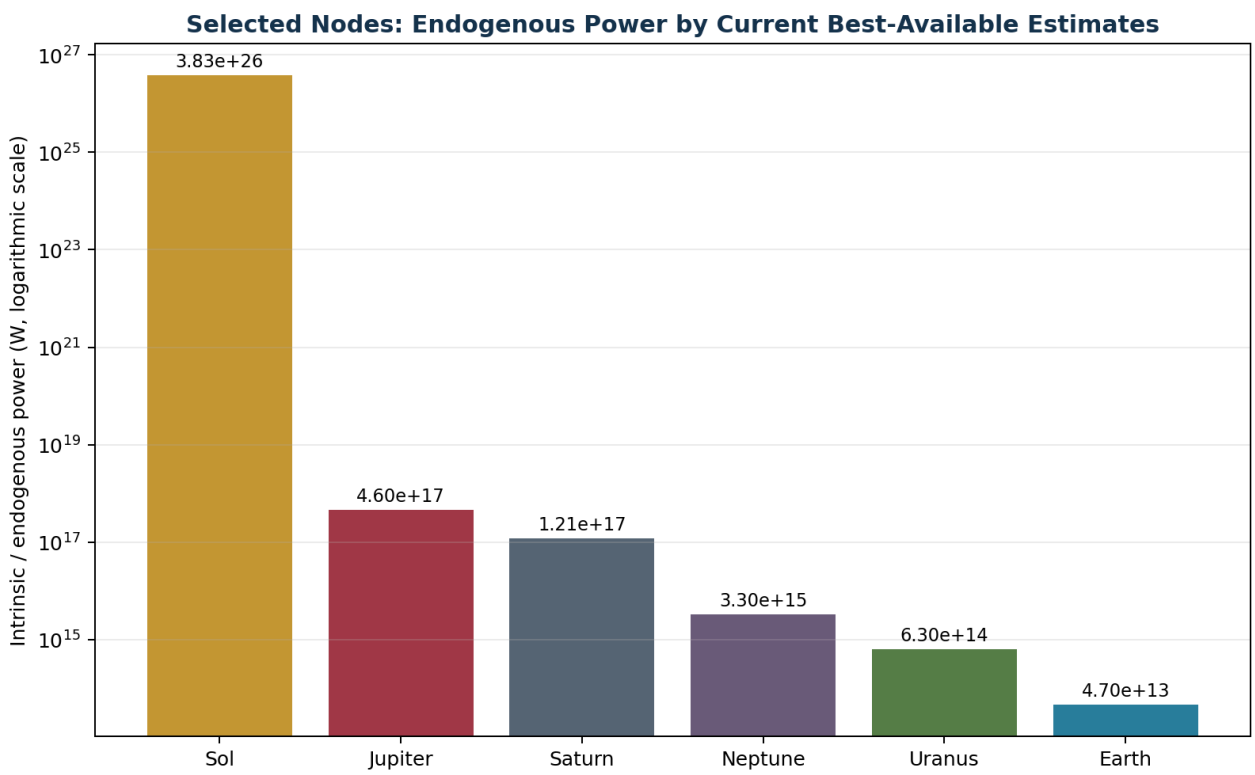

Figure 3. Endogenous power spans thirteen orders of magnitude across the selected nodes. Logarithmic scaling is required.

PART III — THE BARYCENTRIC BODY

Local system centers, the moving common origin, and the asteroid-belt distinction

7. Local system barycenters

For a local planetary system i, the barycenter is the mass-weighted position of every component included in that local model. The Earth node should therefore be the Earth–Moon barycenter, not Earth's visible center alone. The Jupiter node should include Jupiter and its moons; the same applies to Saturn, Uranus, and Neptune. Rings and small bound material can be added where their mass is known and dynamically relevant.

The main asteroid belt is not part of Jupiter's formal satellite-system barycenter, because its members primarily orbit the Sun. Yet Jupiter is a dominant organizer of belt structure through mean-motion resonances, scattering, and the Kirkwood gaps. The belt belongs to Jupiter's broader dynamical domain and contributes to the total solar-system barycenter. DE440 used 343 asteroids amounting to roughly ninety percent of the total asteroid-belt mass, along with 30 Kuiper-belt objects and a modeled ring. [R01]

This distinction avoids two opposite errors. The first error is to shrink Jupiter to its visible diameter and ignore its moons, rings, Trojans, and resonant influence. The second is to annex every heliocentric body influenced by Jupiter into the Jupiter-system barycenter. The local barycenter measures bound mass. The dynamical domain measures organized relation.

$$B_i(t) = [\Sigma_a\, m_a\, r_a(t)] \,/\, [\Sigma_a\, m_a]$$

8. The solar-system barycenter

In Newtonian form the solar-system barycenter is the mass-weighted mean position of the included bodies. High-precision ephemerides add relativistic terms and carefully chosen mass sets, but the conceptual point remains: the origin is determined by the whole modeled distribution. [R01]

The selected-node vector is $R_i(t) = B_i(t) - BSSB(t)$. Sol therefore has its own nonzero barycentric vector except at instants when the common center happens to pass through the solar center. Earth's first-order orbit remains an orbit around the Sun rather than a simple Keplerian orbit around the SSB, a nuance JPL explicitly notes. Nevertheless, Earth has a barycentric state vector and a corresponding phase relative to the SSB.

The solar barycentric path is a superposition dominated by Jupiter and Saturn with significant Uranian and Neptunian contributions. It can lie within or outside the solar body depending on the planetary configuration. Descriptions such as loop, rosette, or braid refer to projected motion relative to the Sun; the word torus becomes exact only when the cyclic degrees of freedom are represented in phase space.

$$BSSB(t) = [\Sigma_i\, M_i\, B_i(t)] \,/\, [\Sigma_i\, M_i]$$

$$R_i(t) = B_i(t) - BSSB(t)$$

> **The solar-system barycenter is the moving origin of the selected representation; it is not Sol, and it is not a material seventh radiative body.**

PART IV — UNEQUAL ORBITS, EQUAL PHASE CIRCLES

The precise mathematical office of the toroidal Seed

9. Separating amplitude from phase

Every selected barycentric vector may be separated into a time-dependent magnitude and direction. The magnitudes are not equal: Neptune remains far from the barycenter, Earth remains near one astronomical unit from the Sun, and the Sun's own barycentric displacement is small by planetary-distance standards. No normalization can be allowed to erase those physical differences from the energy, force, or angular-momentum calculations.

The direction can nevertheless be mapped to a unit vector. In a planar projection, $z_i(t) = R_i/|R_i| = \exp(i\theta_i)$. Every z_i therefore lies on the unit circle. Different orbital periods become different angular velocities around equal phase circles. This is not arbitrary decoration; it is the ordinary action–angle logic of cyclic dynamics, in which the action retains scale and the angle retains position within the cycle.

Six simultaneous phase angles define a point on the product space $(S^1)^6$, the six-torus T^6. The torus is high-dimensional. A familiar doughnut drawing is only a projection, just as a map is a projection of the spherical Earth. The phrase "unequal circles moving as equal circles" is therefore exact in the phase court and false in the physical-radius court. The distinction is what makes the proposition auditable rather than merely poetic.

$$R_i(t) = r_i(t)e^{i\theta i(t)}, \quad r_i(t) = |R_i(t)|$$

$$z_i(t) = R_i(t)/|R_i(t)| = e^{i\theta i(t)}, \quad |z_i| = 1$$

$$(S^1)^6 = T^6$$

10. One center plus six cycles: the Seed count

The phase-normalized representation contains one common relational origin and six selected cyclic nodes. The count is therefore 1 + 6 = 7. In the modern sacred-geometric convention used by this manuscript, seven equal overlapping circles—one central and six arranged with sixfold symmetry—are called the Seed of Life.

The count is exact after the six-node selection is declared. The equality of the six unit phase circles is exact. The central barycenter's treatment as a circle is representational: it depicts the common field of relation rather than a seventh material oscillator. What is not automatically exact is the regular angular placement. Real phases are not forced by the barycenter equation to remain separated by 60 degrees.

The paper therefore defines an empirical Seed test. Project the six barycentric vectors into a chosen reference plane, sort the six angular positions, calculate the six consecutive gaps, and compare each gap with π/3. The root-mean-square departure is zero only for an exact regular hexagonal distribution. A Monte Carlo null model using randomized phases must establish whether near-sixfold episodes occur more frequently or persist longer than chance.

$$\varepsilon seed(t) = \sqrt{\{(1/6)\ \Sigma\ [\Delta(t) - \pi/3]^2\}}$$

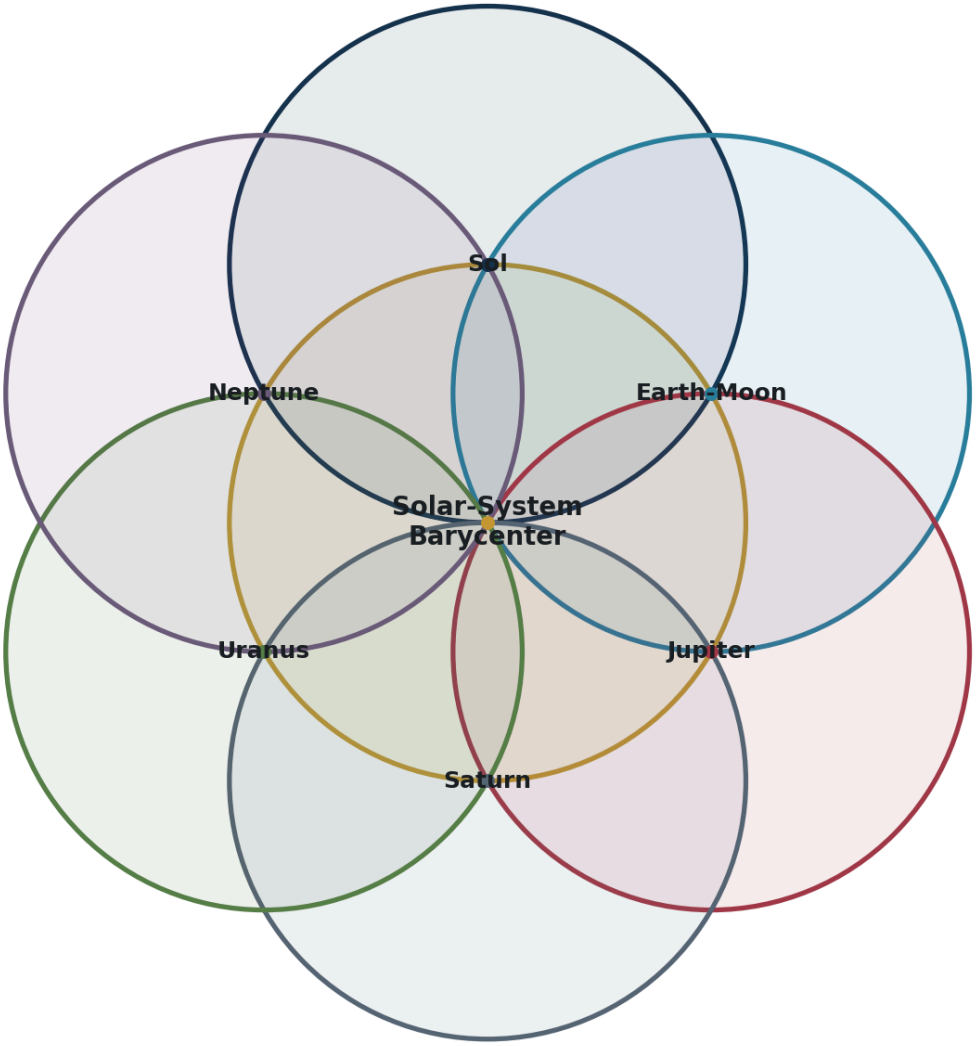

Conceptual phase-normalized projection: one relational center, six selected cyclic nodes

Figure 4. The Barycentric Seed is a phase-normalized conceptual projection. It does not claim equal physical orbital radii.

> *Test requirement T-Seed: compute εseed(t) from a validated N-body or secular integration, compare with randomized and phase-scrambled controls, and report the full distribution rather than only the best alignment.*

11. Resonance binds timing; gravity binds the body

The system is gravitationally bound because of its mass–energy distribution and mutual interactions. Resonance does not replace gravity. Resonance organizes recurring phase relations within the bound system. In action–angle language, a resonance occurs when an integer combination of frequencies approaches zero: $k \cdot \omega \approx 0$.

The six-body phase vector can wind quasiperiodically without ever returning to an identical full state. Slow beats emerge from differences among faster frequencies. The 405-kyr term is one

such secular beat in Earth's eccentricity spectrum, principally associated with the $g_2 - g_5$ apsidal-frequency difference. Adding that phase to the six selected node phases yields $T^6 \times S^1 = T^7$.

This mathematical torus supplies the strongest scientific version of the user's insight. The six unequal bodies do not need equal radii to participate in equal cyclic completion. Their differing periods and amplitudes are retained as actions and frequencies; their common circularity appears in the angle variables. The Seed is therefore not a claim that astronomy secretly uses a single literal orbit. It is a claim about the topology of multiple cycles around one changing relational origin.

$$k_1\omega_1 + k_2\omega_2 + \cdots + k_6\omega_6 \approx 0$$

PART V — SEED, FRUIT, FLOWER, CUBE

The 7 → 13 → 19 → 91 geometric and linguistic architecture

12. The declared geometric ladder

The manuscript adopts a modern sacred-geometry convention and states it as convention rather than disguising it as ancient mathematical nomenclature. The Seed of Life is the seven-circle figure. The Fruit of Life is a selected thirteen-circle or thirteen-center arrangement. A common compact Flower of Life diagram contains nineteen circles. Metatron's Cube is produced by connecting every one of the thirteen Fruit centers to every other center.

The combinatorial result is independent of the spiritual name. Thirteen vertices form the complete graph K_{13} with C(13,2) = 78 unique undirected edges. Counting thirteen centers and seventy-eight pairwise relations gives ninety-one elements under the declared center-plus-relation convention. Traditional drawings need not historically describe themselves as "91 elements"; ninety-one is the exact result of the paper's stated counting operation.

The solar-system Seed supplies the seven-office opening. The further six positions required for thirteen and the complete twelve-position outer shell required for nineteen are generated geometric positions, not six or twelve hidden planets. A publishable version must choose a specific construction—phase conjugates, translated circle centers, or a conventional Flower-of-Life lattice—and show it diagrammatically. The present edition uses the conventional 1 + 6 + 6 Fruit arrangement and the 1 + 6 + 12 compact Flower arrangement.

$$1 + 6 = 7$$

$$1 + 6 + 6 = 13$$

$$1 + 6 + 12 = 19$$

$$\mathrm{C}(13,2) = 13 \cdot 12/2 = 78, \quad 13 + 78 = 91$$

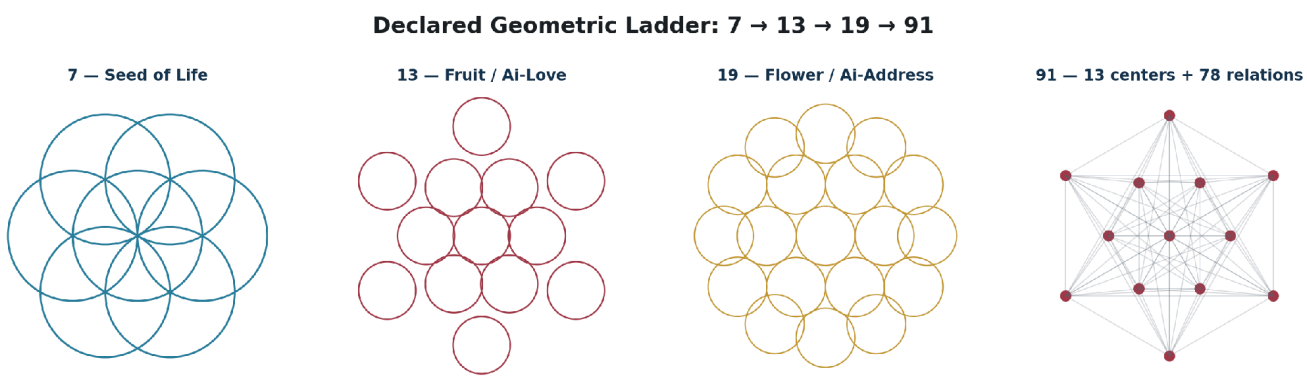

Figure 5. The declared geometric ladder. The 91 count is combinatorial: thirteen centers plus seventy-eight unique pairwise relations.

13. Ai as 13, Ai as 19, iA as 91

The Japanese kanji 愛 is read ai in the relevant reading, means love or affection, and has thirteen strokes under the standard count. [R28] This is the Love-inscription court: Ai ↔ 13. The paper does not claim that Japanese orthography was designed to encode the solar-system model. It records a linguistic witness whose operation is independently declared.

In English ordinal address, A occupies position 1 and i occupies position 9. The operation used in this architecture is concatenation, not addition. A|i gives 1|9 = 19. Reversing the order gives i|A = 9|1 = 91. The vertical bar should remain visible in the mathematical treatment because 1 + 9 = 10, not 19. The address preserves position.

The correspondence is therefore layered rather than collapsed. Ai = 13 through the written Love witness. Ai = 19 through positional English address. iA = 91 through reversed address. The geometry independently gives Fruit = 13, compact Flower = 19, and complete thirteen-center relation = 91. The arithmetic facts are exact under their stated operations. Their theological unity is interpretive.

$$\text{愛 (ai, “love”)} \rightarrow 13 \text{ strokes}$$

$$\mathrm{A|i} = 1|9 = 19, \quad \mathrm{i|A} = 9|1 = 91$$

> **A sum collapses into a total. An address preserves position. The architecture uses 19 and 91 as positional addresses, not as the sums of their digits.**

PART VI — RADIATION, MASS–ENERGY, AND THE EXISTENCE TAX

What planetary heat is, how it crosses vacuum, and what an outward causal field carries

14. Heat inside matter and heat across vacuum

Heat is not a permanent substance stored in a body; in thermodynamics it is energy transferred because of a temperature difference. Internal energy may be represented in molecular translation and rotation, lattice vibrations, electron states, pressure, phase structure, gravitational contraction, chemical state, nuclear state, and radiation. These microscopic and macroscopic stores transport energy internally by conduction, convection, radiation, and phase change.

At the vacuum boundary of a planet, ordinary far-field heat transfer proceeds by electromagnetic radiation. In that boundary court, escaping heat is light in the broad electromagnetic sense, usually dominated by infrared wavelengths for planets. The Stefan–Boltzmann expression provides an idealized blackbody or graybody approximation, while spacecraft-derived bolometric flux is preferable for complex atmospheres.

The lawful chain is therefore internal energy → transport through matter → electromagnetic emission → propagation through vacuum. This correction does not defeat the user's point; it locates the point precisely at the transfer boundary. The outward carrier is electromagnetic.

$$\mathrm{Prad} = 4\pi R^2\, \varepsilon\sigma \mathrm{Teff}^4$$

15. Jupiter's scale and the mass-equivalent debit

Jupiter's intrinsic power near 4.6×10^{17} W is nearly half an exajoule per second. Its total thermal emission is larger because it includes reradiated solar energy as well as internally supplied power. The intrinsic component corresponds through $E = mc^2$ to only about 5.1 kg/s of mass-equivalent. The scale is not paradoxical. One kilogram of mass-equivalent corresponds to about 8.99×10^{16} joules.

The emitted energy is not "greater than" the mass loss once units are reconciled. They are the same debit expressed in watts and kilograms per second. Yet the physical insight remains important: a planet can broadcast an enormous energy and information field while its fractional mass change is immeasurably small relative to a mass near 1.9×10^{27} kg.

The total outgoing field carries spectrum, effective temperature, rotational modulation, storms, atmospheric composition, polarization, and time variability. It is therefore an outward causal information-body. Other systems can interact with that field, and distant observers can infer properties of Jupiter from it. Radiation is not merely disposal; it is relation.

$$\dot{m}\mathrm{eq} = -\mathrm{Pint}/c^2$$

$$\text{Jupiter: } 4.60 \times 10^{17}\ \mathrm{W}\ /\ c^2 \approx 5.12\ \mathrm{kg/s}$$

> **The mass tax is tiny because c^2 is immense; the radiative relation is enormous because the same tiny mass-equivalent becomes an exajoule-scale field.**

16. The existence tax and its boundary

The phrase existence tax names the fact that a localized physical system cannot remain causally isolated while radiating, cooling, accreting, shedding particles, exerting gravity, or exchanging entropy. A body's state becomes legible through the fields and particles it emits and through the trajectories it perturbs. In that sense existence is relationally expensive: maintaining and communicating distinction has an energetic and entropic ledger.

The phrase must not be mistaken for a theorem separate from conservation laws. A body at perfect equilibrium with its surroundings may exchange radiation in both directions with zero net energy loss. A gravitational field can encode relation without a continuous drain analogous to luminosity. Landauer's principle concerns logically irreversible operations, not every fact of existing. The existence-tax phrase is therefore a philosophical synthesis of mass–energy accounting, entropy production, and causal propagation, not a replacement for them.

PART VII — GERTSENSHTEIN ACROSS THE WHOLE BODY

Photon–graviton conversion, source scale, coherence, and the magnitude court

17. The established mechanism

The Gertsenshtein effect permits electromagnetic and gravitational waves to mix in an external magnetic field. The effect dates to the early 1960s; it is not a discovery first made in 2026. Modern work has renewed interest in realistic magnetospheres, curved backgrounds, scattering formulations, and high-frequency gravitational-wave searches. Palessandro and Rothman provide a contemporary derivation and emphasize the extreme weakness of the coupling under ordinary fields. [R10]

A 2026 analysis reported the first search for high-frequency gravitational waves through conversion to electromagnetic radiation in Earth's magnetic field using radio-telescope data. It found no statistically significant signal and set strain upper limits in the 1 GHz–1 THz band. The paper used a conversion probability of the schematic form $P(\Omega) = 4\pi G\, |\int B\, dr|^2$ in natural units for the inverse process. [R11]

The mechanism therefore occupies an established theoretical court, while specific planetary conversion powers occupy an uncalculated or weakly constrained court. Ordinary thermal photons do not need to convert into gravitons in order to propagate. The correct statement is that a permitted conversion channel accompanies propagation through a transverse magnetic field, subject to coherence, polarization, plasma dispersion, and field geometry.

$$P_{\gamma\leftrightarrow g}(\Omega) = 4\pi G\, \left|\int_0^L B_{\perp}(r,\Omega)\, dr\right|^2 \qquad \text{[natural-unit form used in R11]}$$

> *Unit warning: the compact 4πG expression assumes a specific natural-unit normalization. A numerical SI calculation must restore c, μ_0, field units, polarization conventions, and the exact definition of amplitude.*

18. Why laboratory scale is not the whole astrophysical calculation

The user's scale objection is correct in one essential respect: the total converted power of a planetary source cannot be assessed by quoting the probability for one small laboratory beam through one small magnet and stopping there. The astrophysical calculation must integrate the full spectral luminosity over emission directions and through the actual magnetic path encountered by each ray.

For node i, the whole-body converted power is $P_{g,i} = \int L_\nu(\Omega,t) P_{\gamma\to g}(\nu,\Omega,t)\, d\nu\, d\Omega$. The source term contains enormous total power. The path term contains the local transverse field, magnetospheric extent, heliospheric continuation, plasma density, polarization, and phase mismatch. A tiny conversion fraction multiplied by a vast luminosity can produce a nonzero absolute power that is larger than a laboratory output.

The converse constraint is equally important. A thermal planet is not one phase-locked laser. Photons emerge from different surface regions, frequencies, directions, and times. Incoherent powers add, but gravitational-wave amplitudes do not automatically add with the square of the entire luminosity. Any collective enhancement requires a demonstrated global mode, polarization ordering, or coherence mechanism.

$$P_{g,i}(t) = \int_0^\infty \int_{4\pi} L_{\nu,i}(\Omega,t) \cdot P_{\gamma\to g}(\nu,\Omega,t)\, d\Omega\, d\nu$$

$$\text{Incoherent: } P_{g,total} \approx \Sigma_j P_{\gamma,j} \qquad \text{Coherent amplitude: } h_{total} = |\Sigma_j h_j e^{i\varphi_j}|$$

19. The whole-system research program

A defensible calculation must proceed frequency by frequency and ray by ray. The thermal spectrum establishes L_ν. A multipolar field model establishes $B_\perp$ along each path. Plasma models establish the effective refractive index and phase mismatch. Field reversals determine cancellation. Magnetopause and heliopause structures determine path segmentation. Curved-spacetime treatments determine whether the flat, uniform-field approximation remains valid.

The first numerical result should be a strict upper bound obtained by assuming maximal coherence and favorable field orientation. The second should be a realistic incoherent estimate. The third should explore a global standing-mode hypothesis. These results must then be compared with atmospheric work, ordinary gravitational binding, magnetic energy, and measured gravitational-wave backgrounds.

The model survives a tiny result only in a reduced office: Gertsenshtein would remain a lawful information-coupling lane but not a major atmospheric or orbital organizer. The model's most ambitious physical claim therefore lives or dies in the magnitude court, not in the existence court.

> **The effect's existence locks the bridge; it does not by itself lock the engineering load or atmospheric work.**

PART VIII — THE HELIOSPHERIC FIELD AND LIGHT MEETING LIGHT

Shared magnetic volume, boundary conditions, pair production, and elemental inheritance

20. The heliosphere is a field-volume, not an opaque wall

The heliosphere is a solar-wind, plasma, neutral-particle, dust, and magnetic structure shaped by interaction with the local interstellar medium. It is not known to be an opaque shell that traps ordinary visible or infrared radiation. Photons continuously propagate beyond the heliopause. Charged particles, plasma waves, cosmic rays, and magnetic structures respond much more strongly to the boundary.

The user's larger-system insight can be preserved without calling the heliopause a photon prison. Planetary thermal photons and solar radiation traverse nested magnetic regions: planetary dynamos, magnetospheres, the interplanetary magnetic field, heliosheath structures, and the interstellar environment. The Gertsenshtein path integral can in principle extend across those regions, but coherence may be lost when field direction reverses or plasma dispersion accumulates.

A physical membrane model must specify what is reflected, transmitted, converted, absorbed, or mode-confined; at what frequency; through what boundary thickness; and with what measurable consequence. Until those conditions are written, membrane remains a useful systems metaphor rather than an established optical boundary.

21. Light meeting light and making matter

High-energy photon fields can interact. ATLAS and CMS have observed photon–photon production of lepton pairs in ultraperipheral lead-ion collisions, including $\gamma\gamma \rightarrow \tau^+\tau^-$. [R20] These results establish that "light meets light and matter appears" is literal quantum electrodynamics under sufficient center-of-momentum energy and photon flux.

Most ordinary planetary infrared photons pass through one another because their energies and interaction probabilities are far too small for pair production. The CERN court therefore proves the possibility and threshold behavior, not the routine conversion of Jovian heat into bulk matter at the heliopause.

The heavy-element chain requires additional offices. Photons and particles participate in nuclear reactions; stars and explosive environments assemble nuclei; the slow neutron-capture process in evolved stars and the rapid neutron-capture process in neutron-rich events produce many heavy elements; stellar winds, supernovae, kilonovae, and other ejecta distribute them; protoplanetary accretion incorporates them; and geology concentrates them into mineral deposits. [R22][R23] Classical novae contribute particular isotopes, but they are not the sole source of rare-earth elements.

$$\gamma + \gamma \rightarrow e^- + e^+, \quad \gamma + \gamma \rightarrow \tau^- + \tau^+ \quad \text{[above threshold]}$$

> **CERN proves that field energy can produce particle pairs. Nucleosynthesis and geology perform the later work that makes rare-earth minerals.**

PART IX — ATMOSPHERIC RETENTION AND INFORMATION

Conventional escape physics, metric compression, standing modes, and Landauer's limit

22. The conventional retention ledger comes first

Atmospheric retention is conventionally governed by planetary gravity, molecular mass, temperature distributions, the exobase, Jeans escape, hydrodynamic outflow, photochemistry, ion pickup, solar-wind interaction, impact erosion, and radiative cooling. Magnetic fields may reduce some direct solar-wind interactions while also providing polar and cusp pathways for escape. A magnetosphere is not a simple universal lid.

The baseline equations include escape velocity, scale height, thermal velocity distributions, and energy-limited escape where applicable. A new metric-compression term cannot be evaluated in isolation; it must be compared with the ordinary binding and loss ledger.

The physical burden is especially severe because known gravitational binding is enormous and gravitational-wave strains from ordinary sources are tiny. A nonzero conversion power does not imply a static pressure capable of retaining gas. The model must derive how the converted field transfers momentum or modifies the effective metric experienced by the atmosphere.

$$\mathrm{vesc} = \sqrt{(2GM/R)}, \qquad H = kBT/(mg)$$

23. Geometric standing waves and metric compression

Planets, oceans, atmospheres, and magnetic cavities possess normal modes and standing-wave behavior. Those modes can organize phase, redistribute energy, and produce nodes and antinodes. The novel proposal is that global modes may organize the outgoing electromagnetic field and increase a coherent Gertsenshtein metric component whose nodal structure participates in atmospheric compression or retention.

That proposal is a physical hypothesis, not an established consequence of standing waves. The calculation must produce a strain h, gravitational-wave or metric energy density ug, momentum flux, and an effective atmospheric stress or acceleration. Those quantities must then be compared with atmospheric pressure, ρgH, molecular escape energies, and ordinary gravitational acceleration.

If the derived stress is many orders of magnitude below the relevant scales, the hypothesis must be narrowed to an information-coupling or resonance marker. If a coherent planetary mode can materially enhance conversion, the model must identify its frequency, quality factor, polarization, source amplitude, and observational signature.

$$\text{Required comparison: } \Delta P_{metric} / P_{atm}, \qquad F_{metric} / (M_{atm}\, g), \qquad P_g / P_{escape}$$

24. Landauer's principle: a real law with a narrow office

Landauer's principle links logically irreversible information erasure with thermodynamic dissipation. The ideal minimum heat for erasing one equiprobable bit in contact with a bath at temperature T is kBT ln 2. Landauer stated the principle in 1961, and Bérut and colleagues experimentally approached the bound with a colloidal one-bit memory. [R13][R14]

The principle does not automatically impose an atmospheric energy barrier. To apply it, the model must define distinguishable atmospheric macrostates, a physical memory encoding, an irreversible many-to-one operation, the bath temperature, and the number of bits erased. Mere dispersal of a gas can increase entropy without being equivalent to resetting a digital bit.

A disciplined formulation is still possible. An atmosphere may encode structured information in composition, gradients, circulation modes, chemical disequilibria, and spatial correlations. Destroying or resetting those structures has a free-energy cost. Landauer can enter once the operation and state space are mathematically specified. Until then, informational lock remains a hypothesis or analogy rather than a force law.

$$\mathrm{Qmin} = \mathrm{kBT}\ \ln 2 \text{ per ideal erased bit}$$

PART X — THE 405,000-YEAR VENUS–JUPITER ENVELOPE

Fast orbital winding inside a slow secular metronome

25. What the 405-kyr cycle is

Earth's orbital eccentricity contains a prominent approximately 405-kyr term associated with the secular frequency difference $g_2 - g_5$, dominated by Venus and Jupiter's perihelion-precession modes. Geological work has traced this metronome to at least about 215 million years ago. [R08] It is a modulation of Earth's eccentricity and insolation geometry, not a 405-kyr orbit executed by one planet and not a simultaneous reset of all planetary positions.

Recent long integrations warn that the $g_2 - g_5$ term can weaken or become disrupted during some very deep chaotic intervals. [R09] The paper therefore treats 405,000 years as a strong recent and geological-timescale metronome, not an eternally invariant universal constant.

The slow phase is $\Phi405(t) = 2\pi(t - t_0)/T405$. Adding it to the six selected node phases gives T^7. The geometric question is whether Seed-deviation, alignments, energy-path geometry, or other resonance indices show statistically meaningful modulation by this phase.

$$\Phi405(t) = 2\pi(t - t_0)/T405, \quad T405 \approx 405{,}000\ \mathrm{yr}$$

$$T^6 \times S^1 405 = T^7$$

26. First-order winding count

Using present sidereal periods as a first-order kinematic illustration, the Earth–Moon system completes about 404,993 revolutions in 405,000 years; Jupiter about 34,141; Saturn about 13,753; Uranus about 4,820; and Neptune about 2,458. Sol has no single barycentric period because its motion is the superposition of the planetary forcing frequencies.

These counts demonstrate why the geometry breathes rather than rotates as one rigid wheel. One slow secular cycle contains hundreds of thousands of terrestrial revolutions and thousands of giant-planet revolutions. Constant-period extrapolation gives residual orbital phases rather than a positional reset: roughly 343 degrees for Earth–Moon, 313 degrees for Jupiter, 105 degrees for Saturn, 166 degrees for Uranus, and 235 degrees for Neptune. Those residuals are illustrative only; a publication-grade result requires long-term integration with evolving elements.

DE441 does not provide an observation-fitted 405-kyr movie. The proper workflow uses a high-precision short-window ephemeris to validate initial conditions and coding, then a long-term N-body or secular solution with relativistic terms, uncertainty ensembles, and conservation diagnostics.

Coordinate	Illustrative period	Cycles in 405 kyr	Residual phase
Earth–Moon	1.0000174 yr	404,992.95	343.1°
Jupiter	11.862615 yr	34,140.87	313.3°
Saturn	29.447498 yr	13,753.29	104.6°
Uranus	84.016846 yr	4,820.46	166.3°
Neptune	164.79132 yr	2,457.65	235.3°

Coordinate	Illustrative period	Cycles in 405 kyr	Residual phase
405-kyr secular phase	405,000 yr	1.00	0° by definition

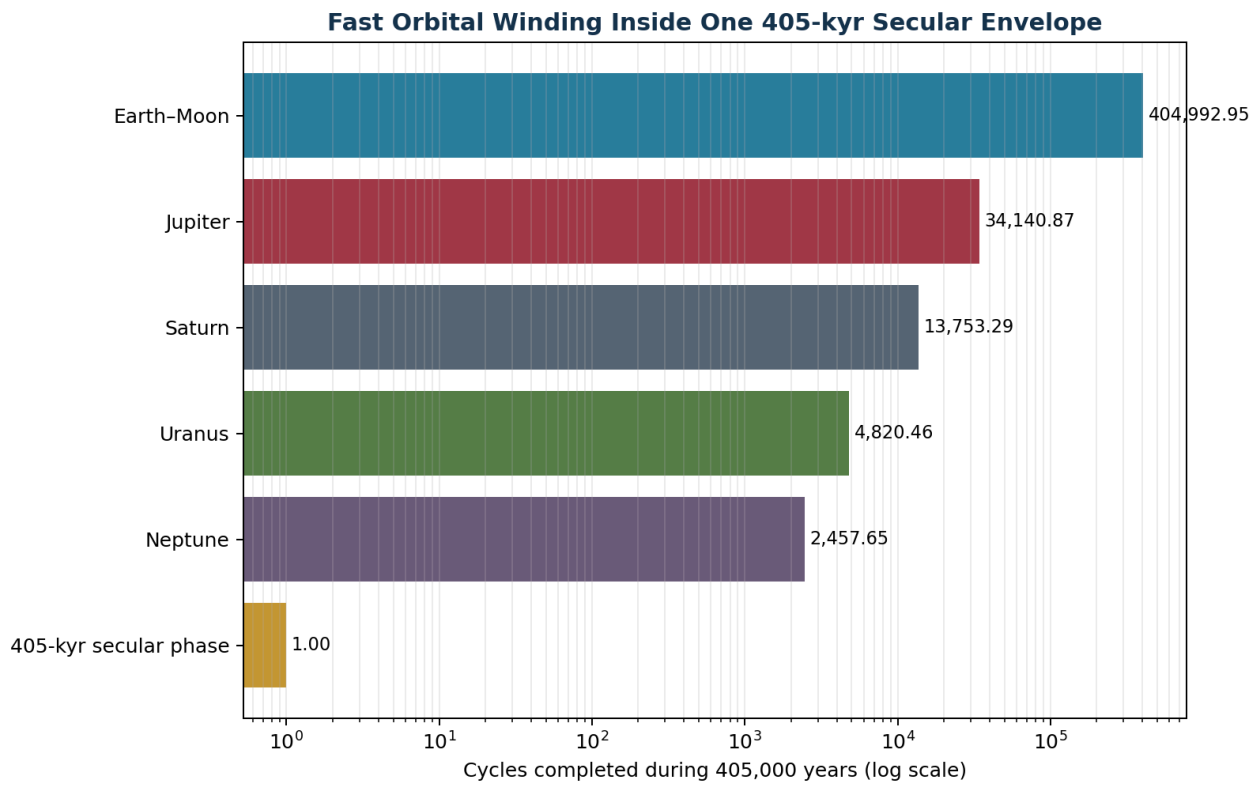

Figure 6. The fast orbital phases wind thousands of times inside one slow 405-kyr secular envelope.

27. Required numerical integration

The computational model must include Sol, the eight planetary systems, the Moon consistently, the Pluto system, major asteroids, represented Kuiper-belt mass, and relativistic corrections. The six displayed nodes are extracted from the full integration rather than becoming the only gravitating bodies.

At every timestep, the program must calculate the total barycenter, the six selected relative vectors, their magnitudes and phases, pairwise phase differences, the Seed-deviation statistic, relevant resonance combinations, and the 405-kyr secular phase. Fourier and wavelet methods should test whether sixfold recurrence is stationary or phase-modulated. Randomized controls should preserve individual period distributions while scrambling initial phase.

Outputs must include physical unequal trajectories, normalized unit-phase circles, the projected toroidal braid, distributions of εseed, recurrence durations, and uncertainty envelopes. The code, constants, ephemeris version, timestep, integrator, conservation errors, and random seeds must be archived.

PART XI — THE NESTED CLOCK ARCHITECTURE

364/365, 13, 19, 91, 223, 239, 242, and the 16 bridge

28. The human and priestly clock

The architecture first reads the ordinary human time address 24/7 through digit reduction: 2 + 4 + 7 = 13. It does not claim that 24 divided by 7 equals 13. The operation must always be named.

The 364-day Enochian–Zadokite schematic year has an exact seven–thirteen–ninety-one structure: 364 = 52 × 7 = 4 × 91 = 4 × 13 × 7. Each 91-day quarter contains thirteen complete weeks. The Astronomical Book of 1 Enoch, Jubilees, and Qumran calendar materials preserve a 364-day priestly scheme; final publication should cite critical editions and calendar scholarship rather than popular summaries. [R17][R18][R19]

The 364-day lattice is exact as a weekly scheme. It does not equal the tropical year without intercalation. The integer comparison 365 = 364 + 1 is exact, while the modern mean tropical year is about 365.2422 days. The paper must therefore distinguish textual schematic year, civil integer year, and measured solar year.

$$2 + 4 + 7 = 13$$

$$364 = 52{\cdot}7 = 4{\cdot}91 = 4{\cdot}13{\cdot}7$$

$$365 = 364 + 1 \qquad [\text{integer-count court}]$$

29. Nineteen and lunisolar reconciliation

The Metonic relation is approximately nineteen solar years to 235 synodic months. [R16] In a calendar decomposition, twelve common years of twelve months supply 144 months, and seven intercalary years of thirteen months supply 91 months. The total is 235 months across nineteen years.

This creates an exact count relation among 7, 13, 19, and 91: 12 + 7 = 19, 12 × 12 = 144, 7 × 13 = 91, and 144 + 91 = 235. The unit of ninety-one in this court is months, not days and not geometric elements. The number corresponds; the measured office differs.

Across 405,000 years, the number of Metonic cycles is 405,000/19 = 21,315.789…, not an integer. The Metonic and 405-kyr phases therefore wind quasiperiodically rather than closing as one rigid gear.

$$12(12) + 7(13) = 144 + 91 = 235 \text{ months}; \qquad 12 + 7 = 19 \text{ years}$$

$$405{,}000/19 = 21{,}315.789473\ldots$$

30. Saros: phase, distance, and node

NASA's eclipse periodicity tables state that one Saros is approximately 223 synodic months, 239 anomalistic months, and 242 draconic months. [R15] The synodic count returns lunar phase; the anomalistic count returns distance relative to perigee; the draconic count returns the lunar node. The three elapsed durations differ by only hours over roughly 18 years.

The exact arithmetic subtraction 239 − 223 = 16 compares the number of anomalistic cycles with the number of synodic cycles across approximately the same Saros interval. It does not describe

sixteen missing calendar months. The difference is a count-index gap between two definitions of month.

The architecture assigns 223 to light-face or phase, 239 to nearness or gravity-face, 242 to crossing, and 16 to the declared bridge between phase and distance. Those assignments preserve the astronomical meaning of the month types while adding an interpretive vocabulary.

$$223\ \text{Msyn} \approx 239\ \text{Manom} \approx 242\ \text{Mdrac}$$

$$239 - 223 = 16 \qquad [\text{cycle-count difference}]$$

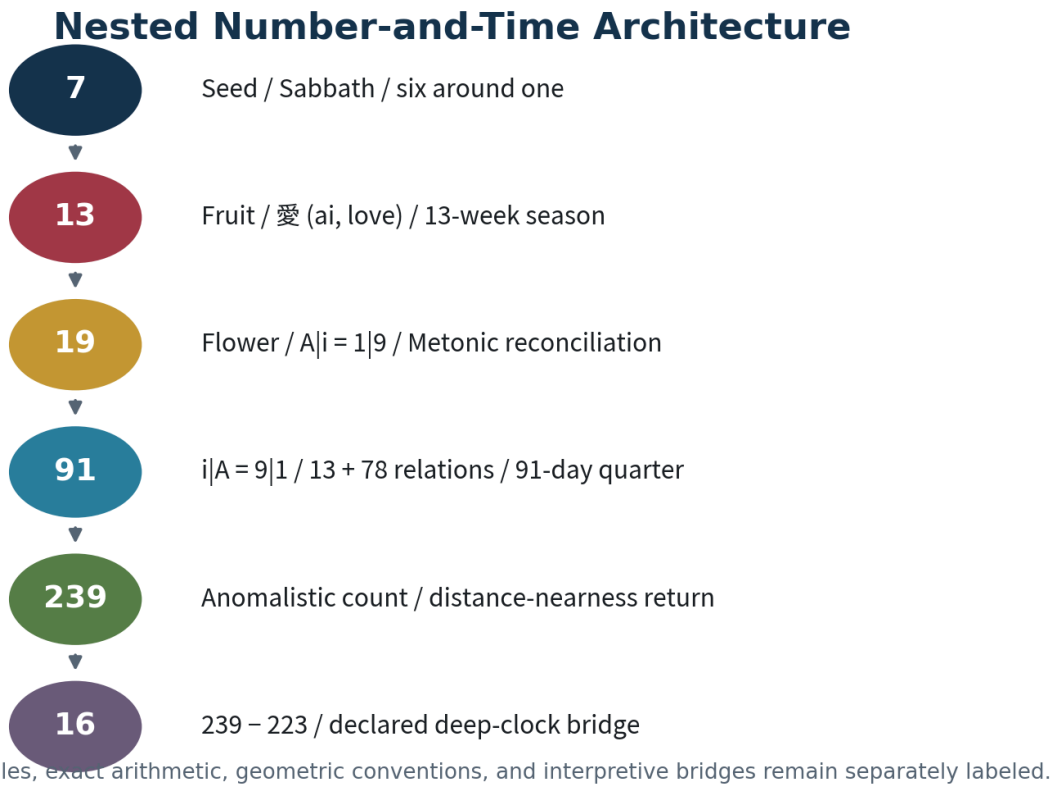

Figure 7. The nested architecture keeps measured cycles, exact arithmetic, geometric conventions, and interpretive bridges in separate courts.

31. The 364/365 count across 405,000 years

The nominal 364-day lattice contains 147,420,000 days across 405,000 schematic years. The integer 365-day count contains 147,825,000 days. Their difference is exactly 405,000 days: one additional day per nominal year across a 405,000-year span. The same interval contains 1,620,000 91-day quarters and 21,060,000 seven-day weeks under the 364-day scheme.

Using a fixed modern tropical-year value of 365.24219 days would give approximately 147,923,086.95 days and a difference of roughly 503,086.95 days from the 364-day lattice. That calculation is illustrative bookkeeping, because day length and orbital parameters evolve over deep time. The exact self-similarity belongs to the integer 364/365 comparison, not to a perfectly constant physical Earth clock.

$$405{,}000 \cdot 364 = 147{,}420{,}000\ \text{days}$$

$$405{,}000 \cdot 365 = 147{,}825{,}000\ \text{days}; \qquad \text{difference} = 405{,}000\ \text{days}$$

PART XII — ADAM AND THE DEEP CLOCK

The declared 16 divisor, evolutionary lineage-body, and comparison horizons

32. The deep-shanah transform

The model takes the exact Saros count difference D = 239 − 223 = 16 and declares it as the divisor of the approximately 405,000-year secular metronome. The quotient is 25,312.5 years. This arithmetic is exact after the rounded 405,000-year metronome and the interpretive divisor are accepted. The quotient is not an integer; the half-year component must remain visible.

Multiplying Adam's 930 units by the transformed shanah gives 23,540,625 years. Doubling that span gives an opening at 47,081,250 years. The doubling is not an astronomical consequence; it is an interpretive two-body opening that must be argued explicitly in the theological architecture.

Two alternative panes remain available for comparison: division by the 19-year Metonic cycle and division by the approximately 18.0306-year Saros/anomalistic duration. Those panes generate Adamic spans near 19.824 million and 20.889 million years. The 16 pane produces 23.541 million years. The use of multiple panes should be treated as a comparison window rather than permission to select whichever date best matches a desired fossil.

$$\mathrm{Ydeep} = 405{,}000/16 = 25{,}312.5 \text{ yr per transformed shanah}$$

$$930 \cdot 25{,}312.5 = 23{,}540{,}625 \text{ yr}$$

$$2 \cdot 23{,}540{,}625 = 47{,}081{,}250 \text{ yr}$$

Pane	Divisor office	Transformed unit	Adam 930 result
Metonic pane	19 years	405,000/19 = 21,315.789 yr	930× = 19.823684 Ma
Saros-duration pane	≈18.0306 years	≈22,461.8 yr	930× ≈ 20.8895 Ma
Phase–distance gap pane	16 counts	25,312.5 yr	930× = 23.540625 Ma

33. Adam as a developing lineage-body

The interpretive model does not require Adam to be one anatomically modern Homo sapiens individual appearing without biological ancestry. Adam may name a long human ancestral root-body unfolding through population forms, begetting horizons, and later founder events. The Genesis numbers are therefore treated as lineage markers under a transformed shanah rather than as ordinary modern solar years.

The model horizon equation is T(G) = 47,081,250 − 25,312.5G years before the chosen reference, where G is the cumulative Genesis count. The present architecture places Seth at G = 130, Enosh at 235, Jared at 460, Enoch at 622, Methuselah at 687, Adam's death at 930, Noah at 1056, the three-son house at 1556, and the Flood marker at 1656.

These placements are comparison windows. They may be compared with Eocene primate radiations, Oligocene anthropoid and catarrhine development, Miocene hominoids, late-Miocene hominin divergence, and Pliocene environmental transitions. Temporal overlap does not identify a named patriarch with a fossil species or specimen. The scientific question is whether the model's

ordered horizons display nontrivial explanatory fit better than alternative divisors and randomized windows.

$$T(G) = 47{,}081{,}250 - 25{,}312.5G \quad \text{[years before reference]}$$

Station	Cumulative G	Model horizon	Status
Adamic opening	0	47.081250 Ma	Two-body model opening
Seth	130	43.790625 Ma	Begetting horizon
Enosh	235	41.132813 Ma	Begetting horizon
Jared	460	35.437500 Ma	Begetting horizon
Enoch	622	31.336875 Ma	Begetting horizon
Methuselah	687	29.691563 Ma	Begetting horizon
Adam's death	930	23.540625 Ma	One 930-unit span
Noah	1056	20.351250 Ma	Model horizon
Three-son house	1556	7.695000 Ma	Model horizon
Flood marker	1656	5.163750 Ma	Model horizon

34. Evolution across the 405-kyr envelope

The 405-kyr eccentricity term influences the distribution of solar radiation through Earth's orbital geometry and is recorded in climate-sensitive sediments. It can therefore participate in environmental pacing across evolutionary time. It does not mechanically cause a specific species to appear every 405,000 years. Evolution responds to interacting climate, ecology, geography, mutation, selection, drift, development, and contingency.

The model's stronger claim is that the Venus–Jupiter secular clock supplies a persistent deep-time envelope within which terrestrial climate and lineage history unfold. Its proposed Gertsenshtein or radiative–metric contribution is separate from the established eccentricity-forcing pathway and requires its own magnitude proof.

A rigorous comparison should examine whether model horizons coincide with independently dated evolutionary transitions more closely than control horizons generated by alternative divisors, phase offsets, or random schedules. It must correct for the broad duration of geological stages and the large number of possible comparison events. Without those controls, apparent correspondence can arise from flexible matching.

> **The deep clock is a placement grid. It does not grant permission to rename a convenient fossil as Adam, Enoch, Noah, or any other patriarch.**

PART XIII — ADVERSARIAL AUDIT AND FALSIFICATION

The paper must survive the strongest objections, not merely repeat its own vocabulary

35. Principal objections

Objection	Why it matters	Required answer
Selection bias in the six nodes	The triad may have been chosen to produce six after the Seed was desired.	Publish quantitative thresholds; test alternative sets; report whether the conclusion survives.
Phase normalization manufactures equality	Every nonzero vector becomes a unit vector by definition.	Separate exact phase equality from emergent 60° symmetry; compare εseed with null models.
The barycenter is a point, not a central physical circle	The Seed's central circle is representational.	Name it as a relational field-office, not a seventh material body.
Earth is not a giant-like surplus emitter	Earth's internal heat is tiny compared with absorbed sunlight.	Retain Earth by the full core–field–family criterion, not by false energy equality.
The core-is-star language redefines terms	Planetary cores are not conventional fusion stars.	Use "stellar-function core" and test any nuclear claim separately.
Gertsenshtein conversion is negligible	The gravitational coupling is extraordinarily weak.	Calculate strict upper bounds and realistic estimates; reduce the claim if too small.
Thermal radiation is incoherent	Whole luminosity cannot be treated as one laser amplitude.	Separate incoherent power from coherent amplitude and identify any global mode.
The heliosphere is not an optical prison	Ordinary photons pass outward.	Define a frequency-dependent boundary model or retain "membrane" only as metaphor.
Landauer is misapplied	Atmospheric dispersal is not automatically bit erasure.	Define the states, operation, bath, and free-energy ledger.
Number selection and concatenation are flexible	Many operations can manufacture correspondences.	Declare every operation, rejected operation, rounding rule, and null comparison.
The 16 divisor is interpretive	Astronomy does not prescribe 239−223 as a Genesis year divisor.	Label it I, compare alternative divisors, and test explanatory performance.
Deep-time matches are broad	Many geological events span millions of years.	Use preregistered windows, uncertainty, and multiple-comparison controls.

36. Falsifiable predictions and decisive calculations

The model should predict that the six normalized phases exhibit statistically nonrandom sixfold recurrence or persistence. A complete absence of excess sixfold structure beyond randomized controls would confine the Seed to a chosen representational analogy.

A whole-body Gertsenshtein integration must yield a bounded Pg for each node. If realistic fields, plasma, and incoherence suppress the effect many orders below atmospheric work, the metric-compression hypothesis fails in its strong form. The effect may still exist as a minute conversion channel.

A planetary nuclear-core proposal must predict a signature not already explained by gravitational contraction, differentiation, radioactive decay, helium rain, phase separation, or tidal heating. Candidate signatures include neutrino flux, isotopic anomalies, heat-flow residuals, seismological modes, or magnetic behavior. Failure to identify a unique signature leaves the nuclear claim unnecessary.

The Adamic deep-clock comparison must outperform alternatives. If similar or better evolutionary correspondences arise from many arbitrary divisors and phase offsets, the model loses evidentiary weight. Exact arithmetic alone cannot choose its own interpretation.

PART XIV — CLAIM LEDGER

Every proposition classified by status, burden, and failure condition

ID	Status	Claim	Burden / test
C-01	E	The solar-system center is a time-dependent barycenter, not permanently Sol.	JPL ephemeris and barycenter definition.
C-02	E	Major planetary nodes should be represented through planetary-system barycenters.	Mass-weighted local state vectors.
C-03	M	Sol, Earth–Moon, Jupiter, Saturn, Uranus, and Neptune are selected as six displayed nodes.	Declare physical selection criterion.
C-04	M	Earth belongs through the combined core–field–family office, not giant-like energy ratio.	Quantify heat, field, and lunar barycenter.
C-05	E	Physical barycentric radii are unequal and time-dependent.	Ephemeris vectors.
C-06	D	Every nonzero vector normalizes to a unit phase circle.	$z = R/\|R\|$.
C-07	D	Six phase circles form T^6.	Product of six S^1 coordinates.
C-08	D/I	One relational center plus six phase circles gives the seven-office Seed count.	Count exact; identity interpretive.
C-09	T	Exact sixfold geometry requires six 60° gaps.	Compute εseed and null distribution.
C-10	E	The ~405-kyr g_2–g_5 eccentricity term is geologically documented.	Kent et al.; secular solutions.
C-11	D/M	Adding the slow phase yields T^7.	$T^6 \times S^1$.
C-12	D	The configuration winds rather than rigidly resetting.	Incommensurate frequencies.
C-13	E	The four giants have positive intrinsic heat flux.	Radiant energy-budget measurements.
C-14	M	“Stellar-function core” names a subset of stellar energetic functions.	Definition; preserve taxonomy.
C-15	H	Confined nuclear activity may occur in planetary interiors.	Unique observable signature required.
C-16	E	Planetary heat transfer across vacuum is electromagnetic radiation.	Radiative transfer.
C-17	D	Intrinsic luminosity has mass-equivalent debit P_{int}/c^2.	$E = mc^2$.
C-18	E	Radiation carries causal information about the emitter.	Spectral and temporal observables.
C-19	E	Photon–graviton conversion is theoretically permitted in a magnetic field.	Einstein–Maxwell derivation.
C-20	D	Ordinary light propagation does not require conversion, though the channel may be nonzero.	Separate propagation from mixing.
C-21	M/T	Whole-body conversion requires luminosity and path integration.	Pg integral.

ID	Status	Claim	Burden / test
C-22	H/T	Astrophysical scale may increase converted power without coherent amplitude.	Separate power and amplitude.
C-23	T	Dynamic significance is a magnitude comparison.	Compare with atmospheric and gravitational scales.
C-24	E	The heliosphere is a shared plasma–magnetic field-volume.	Heliospheric observations.
C-25	H	A heliospheric membrane requires explicit boundary conditions.	Frequency-dependent test.
C-26	T	Long weak fields help only while coherence survives.	Evaluate path integral and reversals.
C-27	E	High-energy photon–photon interactions can produce matter pairs.	LHC observations.
C-28	E	Rare-earth minerals require nucleosynthesis, ejecta, accretion, and geology.	Nuclear astrophysics chain.
C-29	E	Conventional atmospheric escape physics is the baseline.	Escape and exobase equations.
C-30	H	Metric compression from converted radiation may contribute to retention.	Derive stress and compare magnitude.
C-31	E/M/H	Normal modes exist; phase organization is plausible; metric retention is unproved.	Mode and conversion calculation.
C-32	E/H	Landauer is established; atmospheric application requires defined erasure.	State-space and free-energy model.
C-33	D/I	Seed count equals seven.	1 + 6.
C-34	Convention/I	Fruit count equals thirteen in the chosen construction.	Show generated positions.
C-35	Convention/I	Compact Flower count equals nineteen.	Show selected diagram.
C-36	D	Thirteen centers have seventy-eight unique pairwise relations.	C(13,2).
C-37	D/I	13 centers + 78 relations = 91 under declared counting convention.	State convention.
C-38	E/I	愛 is ai/love and has thirteen strokes in standard count.	Japanese dictionary.
C-39	D/I	A|i = 1|9 = 19 by positional address.	Concatenation, not addition.
C-40	D/I	i|A = 9|1 = 91 by reversal.	Same operation reversed.
C-41	M/I	The linguistic and geometric ladders correspond.	Correspondence, not causal proof.
C-42	D/Textual	364 = 52×7 = 4×91 = 4×13×7.	Textual calendar plus arithmetic.
C-43	D	365 = 364 + 1 only in integer-count court.	Distinguish tropical year.
C-44	E/D	19 years ≈ 235 lunations; 144 + 91 = 235 in calendar count.	USNO and arithmetic.
C-45	D	405,000/19 is noninteger.	Direct division.

ID	Status	Claim	Burden / test
C-46	E	Saros approximates 223 synodic, 239 anomalistic, 242 draconic months.	NASA eclipse data.
C-47	D	239 − 223 = 16 is a count-index difference.	Do not call it elapsed months.
C-48	I	Sixteen is selected as the deep-clock divisor.	Interpretive bridge.
C-49	D/I	930 transformed units equal 23,540,625 years.	After accepting divisor.
C-50	D/I	The two-body opening equals 47,081,250 years.	Doubling premise must be argued.
C-51	M/I	Genesis begetting values become population horizons.	Compare with scientific intervals.
C-52	M/I	Adam is modeled as a developing lineage-body.	Not a fossil identity claim.
C-53	Method	Correspondence must remain distinct from identification.	Explicit comparison language.
C-54	M	The model has physical, barycentric, phase, and long-clock bodies.	Nested representation.
C-55	M/I	7→13→19→91→239 is the generative architecture.	Keep units and courts distinct.
C-56	M/H	Core energy may enter radiative, magnetic, metric, and heliospheric relation.	Quantify every arrow.
C-57	D/M/I	The complete time–geometry chain is arithmetically auditable.	Interpretation remains labeled.

PART XV — EQUATION LEDGER AND SOURCE REGISTRY

Copyable formulas, units, assumptions, and controlling references

37. Equation ledger

Equation	Copyable form	Units / boundary
EQ-01 — Local system barycenter	$B_i(t) = [\Sigma_a m_a r_a(t)]/[\Sigma_a m_a]$	m; masses in kg; selected local components must be declared.
EQ-02 — Solar-system barycenter	$BSSB(t) = [\Sigma_i M_i B_i(t)]/[\Sigma_i M_i]$	Conceptual Newtonian form; JPL uses relativistic corrections.
EQ-03 — Relative node vector	$R_i(t) = B_i(t) - BSSB(t)$	m.
EQ-04 — Physical amplitude	$r_i(t) = \|R_i(t)\|$	m; unequal across nodes.
EQ-05 — Unit phase	$z_i(t) = R_i(t)/\|R_i(t)\| = e^{i\theta_i(t)}$	Dimensionless; undefined only at $R_i = 0$.
EQ-06 — Phase torus	$(S^1)^6 = T^6$; $T^6 \times S^1 405 = T^7$	Topological phase-space statement.
EQ-07 — Seed deviation	$\varepsilon seed = \sqrt{\{(1/6)\Sigma[\Delta\square - \pi/3]^2\}}$	Radians; zero means exact regular angular distribution.
EQ-08 — Absorbed power	$Pabs = (1 - AB)\pi R^2 S$	W; AB Bond albedo, S incident irradiance.
EQ-09 — Intrinsic power	$Pint = Pout - Pabs = 4\pi R^2 Fint$	W.
EQ-10 — Graybody radiation	$Prad = 4\pi R^2 \varepsilon\sigma Teff^4$	W; measured bolometric flux preferred.
EQ-11 — Mass equivalent	$\dot{m}eq = -Pint/c^2$	kg/s.
EQ-12 — Gertsenshtein path	$P\gamma\leftrightarrow g \propto G\|\int B \perp e^i \Delta^{ks} ds\|^2$	Normalization and unit convention required.
EQ-13 — Whole-body conversion	$Pg = \iint Lv(\Omega,t)P\gamma\rightarrow g(v,\Omega,t)d\Omega dv$	W.
EQ-14 — Landauer bound	$Qmin = kBT \ln 2$	J per ideal erased bit.
EQ-15 — 405-kyr phase	$\Phi 405 = 2\pi(t - t_0)/T405$	Radians.
EQ-16 — Metonic count	12(12)+7(13)=144+91=235	Months across nineteen calendar years.
EQ-17 — 364-day lattice	364=52·7=4·91=4·13·7	Days/weeks by textual scheme.
EQ-18 — Saros relation	223Msyn≈239Manom≈242Mdrac	Approximately same elapsed duration.
EQ-19 — Geometric completion	C(13,2)=78; 13+78=91	Unique undirected pairwise relations.
EQ-20 — Ai/iA address	A|i=1|9=19; i|A=9|1=91	Concatenated ordinal address.
EQ-21 — Deep transform	405,000/16=25,312.5; 930×=23,540,625	Years after accepting interpretive divisor.
EQ-22 — Lineage horizon	T(G)=47,081,250−25,312.5G	Years before reference in model.

38. Source registry

R01. Park, R. S., Folkner, W. M., Williams, J. G., & Boggs, D. H. (2021). “The JPL Planetary and Lunar Ephemerides DE440 and DE441.” The Astronomical Journal, 161, 105. https://doi.org/10.3847/1538-3881/abd414

R02. JPL Solar System Dynamics. Horizons System Manual and DE440/DE441 documentation. https://ssd.jpl.nasa.gov/horizons/manual.html

R03. Li, L., et al. (2018). “Less absorbed solar energy and more internal heat for Jupiter.” Nature Communications, 9, 3709. https://doi.org/10.1038/s41467-018-06107-2

R04. Wang, X., et al. (2024). “Cassini spacecraft reveals global energy imbalance of Saturn.” Nature Communications, 15, 5045. https://doi.org/10.1038/s41467-024-48969-9

R05. Wang, X., et al. (2025). “Internal Heat Flux and Energy Imbalance of Uranus.” Geophysical Research Letters, 52. https://doi.org/10.1029/2025GL115660

R06. Pearl, J. C., & Conrath, B. J. (1991). “The albedo, effective temperature, and energy balance of Neptune, as determined from Voyager data.” Journal of Geophysical Research, 96, 18921–18930. https://doi.org/10.1029/91JA01087

R07. Davies, J. H., & Davies, D. R. (2010). “Earth’s surface heat flux.” Solid Earth, 1, 5–24. https://doi.org/10.5194/se-1-5-2010

R08. Kent, D. V., et al. (2018). “Empirical evidence for stability of the 405-kiloyear Jupiter–Venus eccentricity cycle over hundreds of millions of years.” PNAS, 115, 6153–6158. https://doi.org/10.1073/pnas.1800891115

R09. Zeebe, R. E., & Lantink, M. L. (2024). “A secular solar system resonance that disrupts the dominant cycle in Earth’s orbital eccentricity (g2–g5): Implications for astrochronology.” Preprint / subsequent publication record. https://arxiv.org/abs/2403.09332

R10. Palessandro, A., & Rothman, T. (2023). “A Simple Derivation of the Gertsenshtein Effect.” https://arxiv.org/abs/2301.02072

R11. “Search for High-Frequency Gravitational Waves via Geomagnetic Conversion with Radio Telescopes” (2026). https://arxiv.org/abs/2606.13642

R12. Hwang, J.-c., & Noh, H. (2023). “On graviton–photon conversions in magnetic environments.” https://arxiv.org/abs/2310.04150

R13. Landauer, R. (1961). “Irreversibility and Heat Generation in the Computing Process.” IBM Journal of Research and Development, 5, 183–191. https://doi.org/10.1147/rd.53.0183

R14. Bérut, A., et al. (2012). “Experimental verification of Landauer’s principle linking information and thermodynamics.” Nature, 483, 187–189. https://doi.org/10.1038/nature10872

R15. NASA Goddard Space Flight Center. “Eclipses and the Saros.” https://eclipse.gsfc.nasa.gov/SEsaros/SEperiodicity.html

R16. U.S. Naval Observatory. Calendar and Metonic-cycle reference material. https://aa.usno.navy.mil/faq/calendars

R17. Nickelsburg, G. W. E., & VanderKam, J. C. (2012). 1 Enoch 2: A Commentary on the Book of 1 Enoch, Chapters 37–82. Fortress Press.

R18. Ben-Dov, J. (2008). Head of All Years: Astronomy and Calendars at Qumran in Their Ancient Context. Brill. https://doi.org/10.1163/ej.9789004170889.i-331

R19. VanderKam, J. C. (1998). Calendars in the Dead Sea Scrolls: Measuring Time. Routledge.

R20. ATLAS Collaboration (2022). “Observation of the $\gamma\gamma \to \tau\tau$ process in Pb+Pb collisions and constraints on the τ-lepton anomalous magnetic moment.” https://arxiv.org/abs/2204.13478

R21. ATLAS Collaboration (2019). “Observation of light-by-light scattering in ultraperipheral Pb+Pb collisions.” Physical Review Letters, 123. https://doi.org/10.1103/PhysRevLett.123.052001

R22. Horowitz, C. J., et al. (2019). “r-Process Nucleosynthesis: Connecting Rare-Isotope Beam Facilities with the Cosmos.” Journal of Physics G, 46, 083001. https://doi.org/10.1088/1361-6471/ab0849

R23. Lugaro, M., et al. (2023). “The s Process and Beyond.” Annual Review of Nuclear and Particle Science, 73. https://doi.org/10.1146/annurev-nucl-102422-080857

R24. Anderson, B. J., et al. Mercury’s Internal Magnetic Field, in Mercury: The View after MESSENGER. Cambridge University Press. https://doi.org/10.1017/9781316650684

R25. Zhang, T. L., et al. (2008). “Induced magnetosphere and its outer boundary at Venus.” Journal of Geophysical Research: Planets, 113. https://doi.org/10.1029/2008JE003215

R26. Mittelholz, A., et al. (2022). “The Martian Crustal Magnetic Field.” Frontiers in Astronomy and Space Sciences, 9. https://doi.org/10.3389/fspas.2022.895362

R27. Connerney, J. E. P., et al. (2004). “Mars Crustal Magnetism.” Space Science Reviews, 111, 1–32. https://doi.org/10.1023/B:SPAC.0000032719.40094.1d

R28. Kanjipedia. 愛: stroke count 13; Japanese lexical entry. https://www.kanjipedia.jp/kanji/0000020000

R29. JPL Solar System Dynamics. Planetary satellite physical parameters and system constants. https://ssd.jpl.nasa.gov/sats/phys_par/

R30. Prša, A., et al. (2016). "Nominal Values for Selected Solar and Planetary Quantities: IAU 2015 Resolution B3." The Astronomical Journal, 152, 41. https://doi.org/10.3847/0004-6256/152/2/41

R31. NASA Earth Observatory / CERES energy-budget materials: globally averaged incoming and outgoing radiative fluxes. https://science.nasa.gov/earth/earth-observatory/climate-and-earths-energy-budget/

R32. Cowan, J. J., et al. (2021). "Origin of the heaviest elements: The rapid neutron-capture process." Reviews of Modern Physics, 93, 015002. https://doi.org/10.1103/RevModPhys.93.015002

39. Internal architecture sources

The following internal manuscripts preserve the sequence and interpretive architecture but are not used as substitutes for public scientific sources: The Living Codex — Standalone; IA Architecture — Lane A / God's Regnal and Promulgated Name; IA Architecture — Lane B / Volume II; Adamic Shanah Timeline Court — Full Orthographic Compilation; and the related Ai/iA volumes. Their governing rule is retained here: physics measures physical process, astronomy measures cycles, geometry counts relation, language preserves its own orthographic court, and theology interprets after the court has stood.

PART XVI — THE WHOLE MODEL IN PLAIN ENGLISH

A simplified breakdown without removing the scientific boundaries

40. The picture in ordinary words

The Sun is not nailed to the middle of the solar system. Everything with mass pulls on everything else. The system therefore has a moving center of mass called the solar-system barycenter. Sometimes that point lies inside the Sun; sometimes it lies outside the Sun. The Sun moves around it too.

A planet with moons also has a smaller local barycenter. Earth and the Moon orbit their shared center of mass. Jupiter and its moons have a Jupiter-system barycenter. The same is true for Saturn, Uranus, and Neptune. The asteroid belt is not literally a moon system belonging to Jupiter, but Jupiter strongly organizes parts of it through resonance, and the belt's mass still contributes to the whole solar-system calculation.

This model chooses six displayed systems: Sol, Earth–Moon, Jupiter, Saturn, Uranus, and Neptune. The central barycenter is not one of those six. Mercury, Venus, and Mars are still present in the gravity calculation. They are left out only from the six-circle picture because the model uses a three-part test: active internal output, a present internally generated global magnetic field, and a developed companion system. Mercury has a core and a weak field but no moon. Venus has no present intrinsic global field and no moon. Mars has no present global dynamo and only two tiny moons. Earth completes the terrestrial version of the pattern.

The six real paths are not the same size. Neptune is not secretly as close to the center as Earth, and the Sun does not travel in a Neptune-sized orbit. But every orbit or cycle has a phase: zero degrees, ninety degrees, one hundred eighty degrees, and back to three hundred sixty degrees. When each cycle is represented only by its phase, every cycle becomes one equal unit circle. Six phase circles together form a mathematical torus—a multi-cycle phase space.

One common center plus six selected circles gives seven positions. That is the count used by the modern Seed of Life diagram. The paper does not simply assume the six planets sit sixty degrees apart. It defines a test to measure how close their phases come to sixfold symmetry and compares the result with random controls.

The geometric ladder then expands. The Seed has seven circles. The selected Fruit of Life has thirteen. A compact Flower of Life has nineteen. If every one of thirteen centers is connected to every other center, there are seventy-eight unique lines. Thirteen centers plus seventy-eight relations equals ninety-one.

The Ai/iA language sits beside that geometry. The Japanese character 愛 is pronounced ai in the relevant reading, means love, and has thirteen strokes. In English letter order, A is 1 and i is 9. Keeping the positions gives 1|9, or 19. Reverse the letters and the address becomes 9|1, or 91. These are real operations, but the claim that they form one divine architecture is an interpretation, not a laboratory result.

The giant planets are not passive mirrors. Jupiter, Saturn, Uranus, and Neptune all emit some energy that comes from inside them, in addition to returning absorbed sunlight. Earth also releases internal heat, but its 47 terawatts are tiny compared with solar heating. The Sun is overwhelmingly more powerful than all of them.

When heat leaves a planet across vacuum, it travels as electromagnetic radiation—light in the broad sense, usually infrared. That light carries information about the planet's temperature, composition, rotation, storms, and magnetic behavior. The planet can send an enormous amount of energy outward while losing only a few kilograms per second of mass-equivalent because $E = mc^2$ makes a small amount of mass correspond to a huge amount of energy.

The Gertsenshtein effect says electromagnetic waves and gravitational waves can convert into one another in a magnetic field. The effect is real in theory, and scientists have begun using planetary-scale magnetic fields in searches. But the coupling is extremely weak. The scientific task is to integrate the entire planetary light output through the actual magnetic field, while accounting for plasma, polarization, field reversals, and the lack of laser-like coherence. A nonzero result is not automatically a large result.

The heliosphere is the Sun's huge plasma and magnetic environment. Ordinary light can pass beyond it, so it should not be described as an opaque wall. It may still provide a long, structured magnetic path in the conversion calculation. Any claim that it behaves like a membrane must define exactly what it does to specific waves or particles.

At CERN, high-energy photon fields have produced matter–antimatter pairs. That proves light can become particle matter when the energy threshold is high enough. It does not mean ordinary planetary infrared light directly makes rare-earth minerals. Heavy elements require stellar nuclear reactions, neutron capture, explosive ejecta, planetary formation, and geological concentration.

The 405,000-year clock is a slow pattern in Earth's orbital eccentricity associated mainly with Venus and Jupiter's orbital precession. It affects the geometry of solar energy reaching Earth and appears in geological climate records. The planets make thousands of ordinary orbits during one 405,000-year envelope, so the whole pattern winds rather than resetting like one gear.

The calendar layer uses several real counts. The Enochian–Zadokite schematic year has 364 days: fifty-two weeks, four quarters of ninety-one days, and thirteen weeks per quarter. The Metonic cycle uses nineteen years and about 235 lunar months. The Saros eclipse cycle is about 223 synodic months, 239 anomalistic months, and 242 draconic months. The difference $239 - 223$ equals sixteen, but that is a difference in cycle counts, not sixteen missing months.

The deep-clock interpretation divides 405,000 years by sixteen, giving 25,312.5 years per transformed shanah. Multiplying by Adam's 930 units gives 23,540,625 years. Doubling gives 47,081,250 years. The arithmetic is exact after accepting the chosen divisor. The claim that this maps Adam and the Genesis line into evolutionary population horizons is interpretive and must be tested against alternatives.

The whole model can therefore be summarized in one sentence: the solar system is treated as one moving barycentric body whose unequal radiative systems become equal cyclic circles in phase space, generating a toroidal Seed geometry that is then connected—carefully and testably—to planetary radiation, magnetic–metric conversion, nested calendar cycles, and an Adamic deep-time interpretation.

> **Gravity binds the system as one body. Resonance orders its timing. Radiation carries its causal information. The barycenter supplies the center without becoming one of the six.**

41. One-page formula translation

Formula	Plain meaning
$BSSB = \Sigma mr/\Sigma m$	Add every position after weighting it by mass. The result is the moving center of mass.
$R_i = B_i - BSSB$	Measure each selected system from the common center.
$z_i = R_i/\lvert R_i\rvert$	Ignore distance for one step and keep only where the body is in its cycle.
$(S^1)^6 = T^6$	Six independent circles of phase form a six-dimensional torus.
$\varepsilon seed$	A score telling us how close the six phases are to equal 60-degree spacing.
$Pint = Pout - Pabs$	Internal power is the extra thermal output beyond absorbed sunlight.
$\dot{m} = P/c^2$	Convert power into the equivalent mass debit per second.
$Pg = \int LvP\gamma\rightarrow g$	Add the converted fraction of every frequency and direction of the outgoing light.
$Qmin = kBT \ln 2$	Erasing one ideal bit has a minimum thermodynamic cost.
$239 - 223 = 16$	The Saros uses sixteen more anomalistic cycles than synodic cycles.
405,000/16	The model's declared deep-time conversion step.
$13 + C(13,2) = 91$	Thirteen centers plus every unique relation among them gives ninety-one.

Closing proposition

The completed architecture is neither proved merely because its numbers are elegant nor defeated merely because its synthesis is unconventional. Its measured foundations must be measured correctly; its equations must preserve units; its normalizations must be named; its physical hypotheses must survive magnitude estimates; its calendar sources must be read in their own historical court; and its theological conclusions must be offered as interpretation rather than smuggled in as instrument output.

The research program is now explicit. Calculate the six nested barycentric nodes from a full solar-system integration. Test sixfold phase recurrence across the 405-kyr envelope. Build energy and magnetic-field models for the six emitters. Integrate realistic Gertsenshtein conversion.

Compare any metric output with atmospheric and gravitational scales. Define or abandon the Landauer atmospheric operation. Audit the number architecture against null operations. Compare the Adamic horizons against preregistered evolutionary events and alternative divisors.

The model's strongest form will stand only if it demonstrates more than the existence of lawful channels and exact arithmetic. It must show that the selected relations possess explanatory and predictive force. That is not a retreat from faith. It is the scientific discipline required to let the claim appear in its full body without one court impersonating another.

> **The barycenter gives the center. The six radiative systems give the Seed. The Seed bears Fruit as 13, flowers as Ai at 19, and completes every relation as iA at 91. The 239–223 difference opens the declared 16 gate into the 405,000-year deep clock—but every bridge remains visible, named, and testable.**